DEFENCE RESEARCH ESTABLISHMENT
CENTRE DE RECHERCHES POUR LA DÉFENSE
VALCARTIER, QUÉBEC

DREV-TM-1999-088
Unlimited Distribution / Distribution illimitée

BOUNDARY LAYER SURVEY ON A MODEL OF A SPARROW AIM-7M MISSILE IN THE DREV TRISONIC WIND TUNNEL

by

E. Y. Fournier

December/décembre 1999

Approved by / approuvé par

Head, Delivery Systems Section
Chef, Section systèmes de lancement

13 Dec. 99
Date

WARNING NOTICE

The information contained herein is proprietary to Her Majesty and is provided to the recipient on the understanding that it will be used for information and evaluation purposes only. Any commercial use, including use for manufacture, is prohibited. Release to third parties of this publication or of information contained herein is prohibited without the prior written consent of DND Canada.

© Her Majesty the Queen in Right of Canada as represented by the Minister of National Defence, 1999

101-02369/

ABSTRACT

The present wind tunnel investigation is part of a project studying the effectiveness of reaction jet controls on missiles and projectiles. As a comparison basis between reaction jets and conventional control appendages was required, a complete database of aerodynamic coefficients and pressure surveys had to be developed on a specific model shape. It was decided to use a model of the Sparrow AIM-7M medium range missile for this purpose as it would also demonstrate the capability of DREV's trisonic wind tunnel in the experimental investigation of actual missiles. Measurement of the boundary layer characteristics in the vicinity of a control wing and of a stability fin were performed in order to compare the body interaction on fins with respect to that of the full scale vehicle. A successful comparison with analytical results for free-flight conditions should allow for good correlation between free-flight and wind tunnel aerodynamic coefficients. The database for the reaction jet project was generated and comparative results have indicated that DREV's trisonic wind tunnel can generate good technical results for missile shaped models.

RÉSUMÉ

La présente série d'essais en soufflerie fait partie d'un projet portant sur l'étude de l'efficacité des jets latéraux pour le contrôle de projectiles et de missiles. Comme le besoin d'une base de comparaison entre les jets latéraux et les méthodes de contrôle conventionnelles était évident, il fut décidé de générer une banque de données sur les coefficients aérodynamiques pour un modèle de missile générique. Cependant, au lieu d'utiliser un missile générique, un modèle du missile à moyenne portée Sparrow AIM-7M fut utilisé, à cause de la grande quantité d'information aérodynamique existant sur ce missile. De plus, l'utilisation d'un missile avec des coefficients aérodynamiques connus allait permettre de démontrer la capacité de la soufflerie trisonique du CRDV d'étudier ce type de corps à long allongement, et avec de grandes surfaces de contrôle. Des mesures de la couche limite approchant les surfaces de contrôle et les ailettes arrières ont été effectuées afin d'évaluer l'interaction du corps du modèle en comparaison au missile pleine grandeur. Une série de comparaisons fructueuses avec des résultats analytiques pour des conditions de vol libre démontre qu'une bonne corrélation devrait exister entre les coefficients aérodynamiques calculés en soufflerie et ceux du missile pleine grandeur en vol libre. La base de données pour le projet des jets latéraux fut générée, et les résultats comparatifs ont démontrés que la soufflerie trisonique du CRDV peut générée de bons résultats techniques pour des modèles de cette forme.

TABLE OF CONTENTS

ABSTRACT / RÉSUMÉ i

TABLE OF CONTENTS iii

EXECUTIVE SUMMARY v

NOMENCLATURE vii

1.0 INTRODUCTION 1

2.0 EXPERIMENTAL SITE AND INSTRUMENTATION 1

3.0 MODELS AND TEST CONDITIONS 2

4.0 RESULTS AND COMPARISONS 5
4.1 Theoretical Development of Boundary Layer Information 5
4.2 Wind Tunnel Results: Mach 2.0 6
4.3 Wind Tunnel Results: Mach 3.0 8

6.0 CONCLUSIONS AND RECOMMENDATIONS 11

7.0 ACKNOWLEDGEMENTS 11

8.0 REFERENCES 12

TABLE I to III

FIGURES 1 to 7

APPENDIX A - Testing Schedule

APPENDIX B - Detailed Drawings of Model

EXECUTIVE SUMMARY

Air-to-air missiles have been part of the Canadian Forces inventory for several decades. At present, the Sidewinder AIM-9 short-range IR missile and the Sparrow AIM-7M medium range missile are the two major components of the Air Force inventory. These missiles use traditional aerodynamic appendages to provide control during their flight. The introduction of reaction/lateral jet control systems (RJC) in the missile industry is presently modifying the role of control appendages as development programs are under way around the world (US, UK, France, and others) to study and use the potential of RJC systems. Reaction jet flight control systems can provide extended improvements in terms of manoeuvrability, response time, and drag. However, a thorough understanding of the complex aerodynamic effects induced by the injection of transverse jets into a supersonic freestream is required before using this new technology in a design phase.

In order to develop a knowledge base and an expertise with this new technology in the field of control systems, the Defence Research Establishment Valcartier (DREV) has been involved in a research project to study the aerodynamic performance of vehicles guided by reaction jet controls. The specific objective of this study is to improve our understanding of the possible threat posed from weapons using these systems and to exploit this new technology in our own development efforts. The overall research project involves numerical studies, wind tunnel investigations and free-flight firings of various configurations of vehicles. The present phase of the project involved the development of an aerodynamic coefficient database and a study of the boundary layer characteristics about a generic missile with appendages, to serve as a baseline performance comparison with this new control technology. In order to also evaluate the capacity of the DREV wind tunnel in generating accurate results for missile testing, an actual missile, the Sparrow AIM-7M, was selected as the baseline model.

The present investigation is composed of a wind tunnel experiment to measure forces and boundary layer characteristics on a scaled-down model (approximately 15% of the original dimensions) of the Sparrow AIM-7M air-to-air missile. The results from the forces and moments study have been reported in a separate report. Measurement of the boundary layer characteristics in the vicinity of a control wing and of a stability fin were performed in order to compare the body interaction on fins with respect to that of the full scale vehicle. The boundary layer experiments were carried out for nominal Mach numbers 2.0 and 3.0. A successful comparison with analytical results for free-flight conditions should allow for good correlation between free-flight and wind tunnel aerodynamic coefficients.

Comparisons with actual AIM-7F data have shown that DREV's Trisonic Wind Tunnel can provide results comparing well with actual missile bodies. Thus, high l/d bodies with large appendages can successfully be tested in this facility.

NOMENCLATURE

d	Body diameter [m]
H_{12}	Shape factor
l	Body length [m]
N	Power law exponent
R	Model radius [m]
u	Velocity at a distance y from the body surface [m/s]
U_∞	Velocity at the edge of the boundary layer [m/s]
y	Radial distance from model surface [m]
δ	Boundary layer thickness [m]
δ_1	Displacement thickness [m]
δ_2	Momentum thickness [m]
ρ	Density [kg/m^3]
ρ_∞	Freestream density [kg/m^3]

Subscript

∞	Undisturbed flow

1.0 INTRODUCTION

Air-to-air missiles have been part of the Canadian Forces inventory for several decades. At present, the Sidewinder AIM-9 short-range IR missile and the Sparrow AIM-7M medium range missile are the two major components of the Air Force inventory. These missiles use traditional aerodynamic appendages to provide control during their flight. The introduction of reaction/lateral jet control (RJC) systems in the missile industry is presently modifying the role of control appendages as development programs are under way around the world (US, UK, France, and others) to study and use the potential of RJC systems. The present wind tunnel investigation is part of a project studying the effectiveness of reaction jet controls on missiles and projectiles (Ref. 1). As a known base missile configuration was required to allow for performance comparisons, it was decided to use the Sparrow AIM-7M, which has been in service with the Canadian Air Force for several years, and on which experimental aerodynamics data exists. Another important objective behind the use of a known missile is the validation of the DREV wind tunnel for missile aerodynamic studies. High length-to-diameter ratio (l/d) projectiles have previously been tested in this wind tunnel facility, but the use of a high l/d body, with large and multiple control surfaces is a first for this facility.

The present investigation is composed of a wind tunnel experiment to measure forces and boundary layer characteristics on a scaled-down model (approximately 15% of the original dimensions) of the Sparrow AIM-7M air-to-air missile. This memorandum describes the boundary layer experiments carried out for nominal Mach numbers 2.0 and 3.0, at two different locations on the missile. The results from the force and moment study have been reported in a separate report (Ref. 2).

This work was conducted at Defence Research Establishment Valcartier (DREV) between October 1996 and May 1998, under Project 3EB12 - Flight Dynamics for Missile Performance Studies.

2.0 EXPERIMENTAL SITE AND INSTRUMENTATION

The DREV tri-sonic wind tunnel, shown schematically in Fig. 1, is an intermittent, in-draft wind tunnel with a 0.6m x 0.6m test section. Because of its in-draft characteristic (air flowing from an atmospheric pressure tank to a vacuum tank), values of Reynolds numbers are lower than the free-flight values during tests at high Mach numbers. The range of Reynolds numbers for this test series varied between 12.8×10^6 /m (for Mach number = 2.0) and 7.8×10^6 /m (for Mach number = 3.0). Tests were performed at 2 Mach numbers (2.0 and 3.0). The useful duration of testing for these conditions was around 7 seconds.

Boundary layer surveys were conducted at several locations on the model surface to determine the thickness of the boundary layer at these locations (at a fixed angle of incidence of 0°) (see Appendix A for a list of runs).

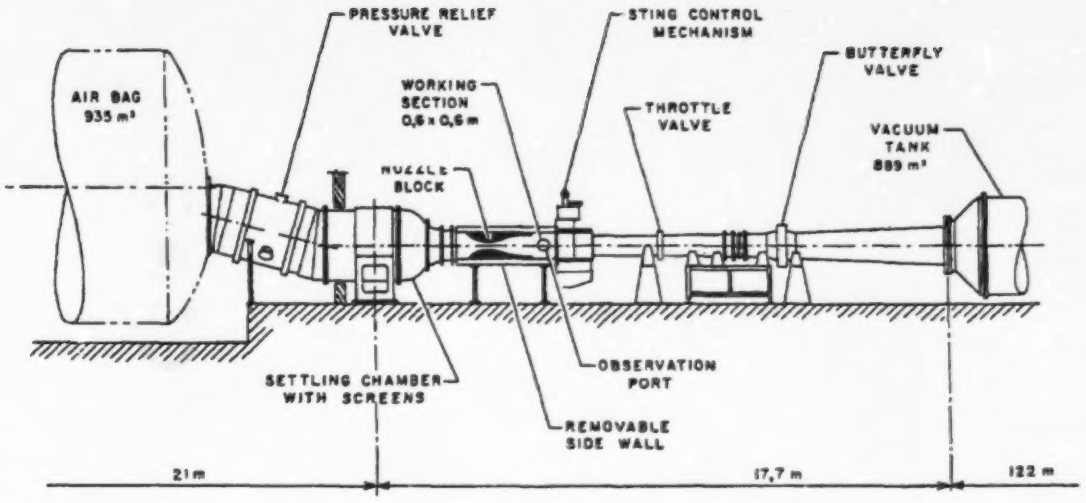

FIGURE 1 – DREV intermittent in-draft wind tunnel

Pressure measurements on the model were obtained by means of electronically scanned ESP pressure modules (Pressure Systems Inc.). The surface pressure taps, providing the local static pressure, were positioned in line with the Pitot tubes. The boundary layer profiles on the missile were obtained by means of a series of "duck beak" Pitot tubes adjusted for a range of previously specified heights. These probes allowed the pressure measurements to be recorded at a distance as small as 0.2 mm from the surface of the model.

Standard instrumentation (wall pressure taps and temperature probes) located in the air bag and in the test section were used to monitor the tunnel free stream conditions. After each run, analog results from the data acquisition instrumentation (including the results from the tare run) were digitized and stored for further transformation through the data reduction software. The data reductions equations will be detailed in the results section of this report.

3.0 MODELS AND TEST CONDITIONS

The missile to be tested is shown in Fig. 2, along with its sting supporting system. A photograph of the model mounted in the wind tunnel is also shown in Fig. 3. It is a 1 to 7 ratio model of the Sparrow AIM-7M air-to-air missile. The AIM-7M missile is controlled by two pairs of wing sets located at about mid length of the missile and stabilized by 4 fins located at the rear of the missile. This model has an ogival nose and a 30 mm diameter cylindrical main body, for a total model length of 531 mm. The l/d of the model is 17.7. The sting to model diameter ratio for this model is 0.677, and the sting length aft of the body is less than 1 caliber before the beginning of the tapered section of the sting.

The boundary layer surveys were performed with the model at 0° angle of incidence, in a "+" wing configuration (roll orientation of 0°) and at two specific locations. The first location, in front of the control wings, is situated at a distance of 6.675 calibers from the nose of the model (where 1 caliber = 1 body diameter). The second location, in front of the fins, is situated at a distance of 14.705 calibers from the nose of the model. For each Mach number, three cases were investigated: survey in front of the control wings, survey in front of a fin without the control wings installed, and survey in front of a fin with the control wing installeds (to identify the interference of the control wings on the boundary layer affecting the fins). Figure 4 shows the control wings and the Pitot probe (duck beak) in position for a survey at a low height position. Figure 5 shows the 2 locations where boundary layer surveys were performed on the surface of the model. A single boundary layer Pitot probe was used for each wind tunnel test. A series of wind tunnel tests was therefore required to obtain the velocity profiles at the two locations (see Appendix A). No attempts were made to disturb the boundary layer during this experiment.

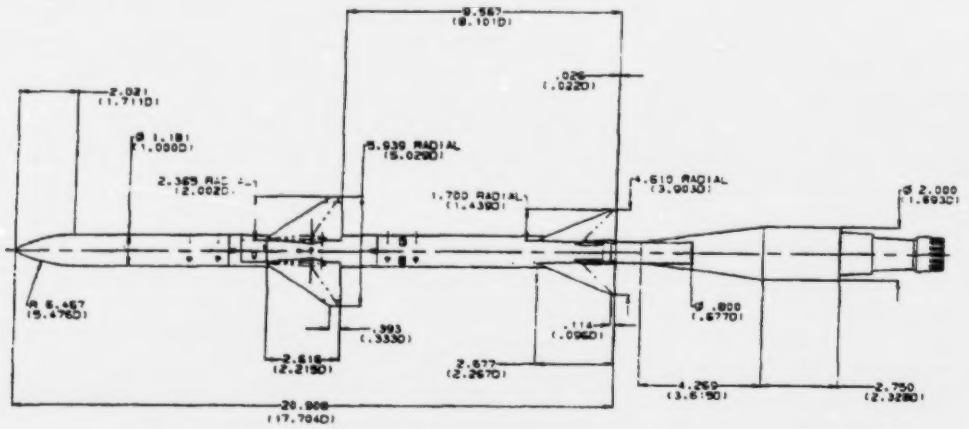

FIGURE 2 - Schematic of the AIM-7M missile model (units: inches (calibers))

This model has been designed and built in 3 modules, to allow for parametric aerodynamic studies of different body configurations. The first module is for the nose of the model, and has a length of 6.24 calibers. The second module is for the mid-section of the missile, and it has a length of 4.43 calibers. This module is used to house the wind tunnel balance during force measurements, and is the section which will be modified in subsequent testing to also house the lateral reaction jet generating system. Three different second modules have been built: one without wings installation set-up (clean body), one with wings installation set-up allowing for odd angles of attack (10°, 30°), and the last one with wings installation set-up allowing for even angles of attack (0°, 20°). Finally, the third module is the tail section of the body and it is 7.03 calibers long. Two versions of this module have been designed and built. The first one is a module with the fixed fins of the Sparrow missile, while the second one is again a body without any fins (clean body). Finally, removable antennas and attachment pins have also been designed. Appendix B shows drawings of various selected model components.

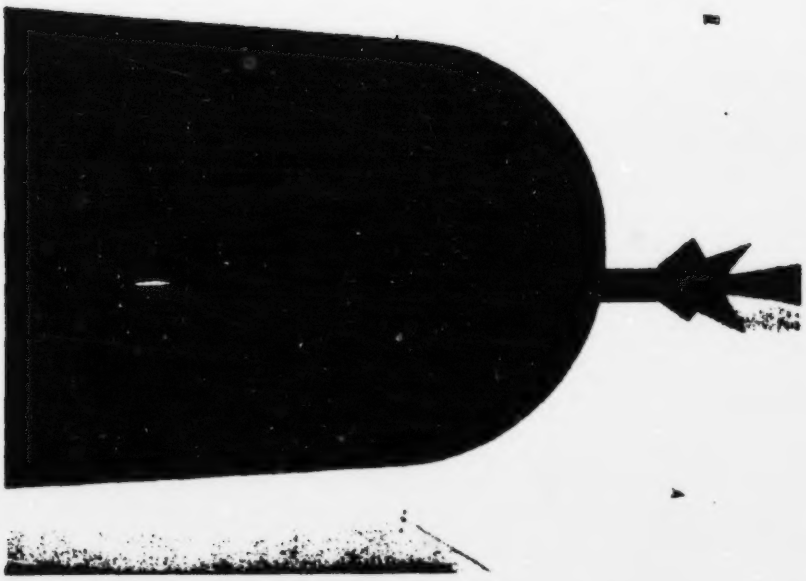

FIGURE 3 - Photograph of the model

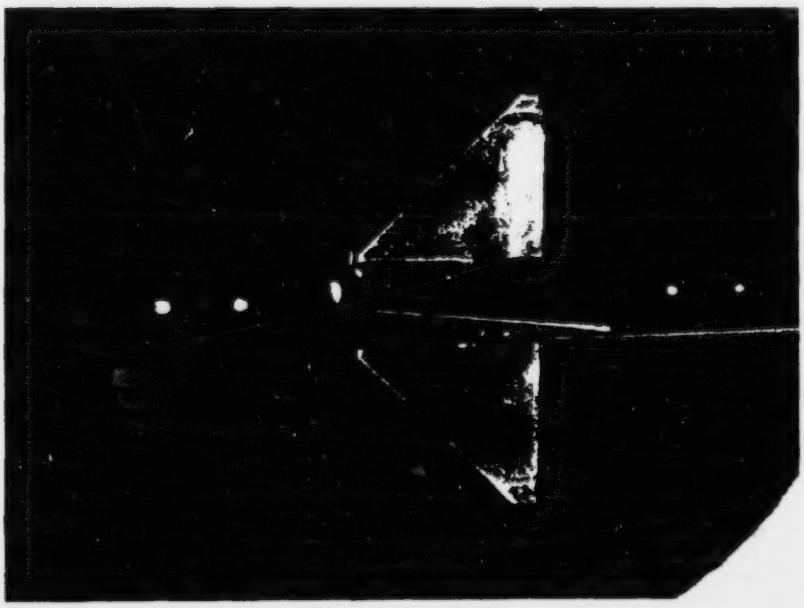

FIGURE 4 – Location of the Pitot probe in front of the control wing
("+" configuration)

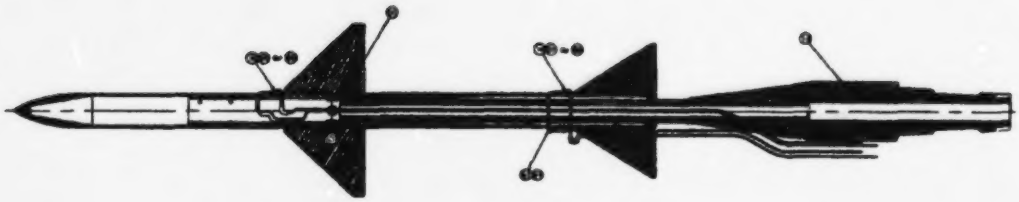

FIGURE 5 – Locations of boundary layer surveys

4.0 RESULTS AND COMPARISONS

4.1 Theoretical Development of Boundary Layer Information

A power law of the form:

$$\frac{u}{U_\infty} = \left(\frac{y}{\delta}\right)^{1/N} \tag{1}$$

is used to express the velocity ratio vertical distribution with respect to the distance to the wall to define a boundary layer (Ref. 3). In this equation, u is the velocity at a distance y from the body surface, and U_∞ is the velocity at the edge of the boundary layer, which is at a distance δ from the surface of the body. The factor N is based on the nature of the boundary layer and varies between 1.4 and 10. Laminar boundary layers are characterized by low values of this factor (between 1.4 and 4.0), while turbulent ones are mostly represented by higher values (5 to 10). The edge of the boundary layer is defined by a distance δ at which the velocity (u) is 0.99 U_∞.

Additional useful information about the boundary layer can be generated. For the present case of a compressible flow about a circular body, two additional characteristics can be defined. The displacement thickness (δ_1) indicates the distance by which the external streamlines are shifted owing to the formation of the boundary layer (Ref. 3) and can be defined as:

$$\delta_1 = \int_0^\delta \left(1 - \frac{\rho}{\rho_\infty}\frac{u}{U_\infty}\right)\left(1 + \frac{y}{R}\right)dy \tag{2}$$

The second characteristic, the momentum thickness (δ_2), is a length associated with the momentum deficit experienced by the flow, because of friction (Ref. 3). It can be defined as:

$$\delta_2 = \int_0^{\delta} \frac{\rho}{\rho_\infty} \frac{u}{U_\infty} \left(1 - \frac{u}{U_\infty}\right) \left(1 + \frac{y}{R}\right) dy \qquad (3)$$

where ρ is the density, ρ_∞ and U_∞ are respectively the free-stream density and velocity, and R is the model radius. The values for these two characteristics are calculated through numerical integration using Simpson triplets non-symmetrical method. From these two definitions, another characteristic, the shape factor (H_{12}), can be defined as:

$$H_{12} = \delta_1 / \delta_2 \qquad (4)$$

and allows one to quantify a given velocity profile. Shape factors for specific conditions have been calculated through direct integration of the above equations (Ref. 4) and typical values are presented in Table I.

TABLE I

Typical values of the shape factor

Mach number	Laminar Boundary Layer	Turbulent Boundary Layer
2.0	5.8	3.0
3.0	9.2	5.0

4.2 Wind Tunnel Results: Mach 2.0

As mentioned previously, boundary layer surveys were performed at two locations on the model. In front of a wing (a distance of 6.675 calibers from the nose tip), and in

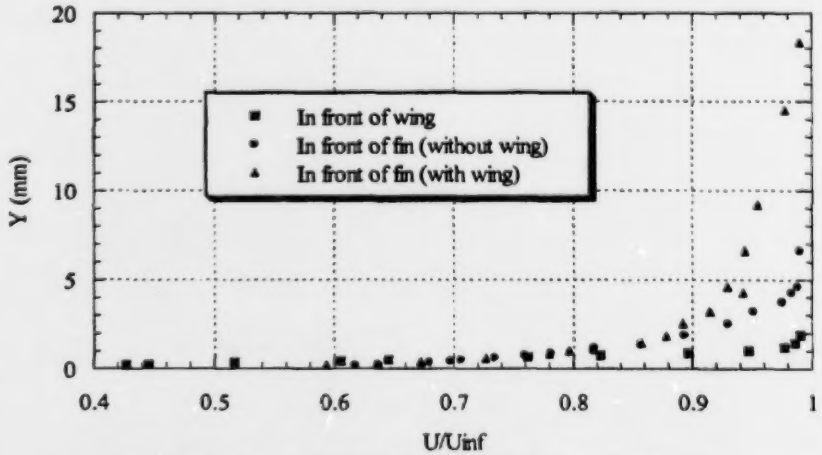

FIGURE 6 – Boundary layer results for Mach 2.0

front of a fin (a distance of 14.705 calibers from the nose tip). From the present wind tunnel conditions (low Reynolds number), and the positions of the boundary layer surveys, it was calculated that the boundary layer would be laminar at the first location, but turbulent at the second location (Ref. 3). The critical Reynolds number used for these calculations, based on the length along the model, is 4.3×10^6. For the first location (laminar), the analytical calculations (Ref. 3) forecasted a boundary layer thickness of the order of 1 to 3 mm.

The data presented in Fig. 6 is for the Mach 2.0 cases (3 sets of data). This information has also been tabulated to allow for easy comparisons. Table II shows various parameters relating to the boundary layer and its development in this high velocity flow.

TABLE II

Boundary layer survey results at Mach 2.0

Parameter	In front of the wing	In front of the fin (without wing)	In front of the fin (both) (with wing)
Boundary layer thickness δ (mm) Experimental	1.91	6.64	18.24
Boundary layer thickness δ (mm) Power Law	1.35	4.46	9.59
Displacement thickness δ_1 (mm)	0.60	1.24	3.43
Momentum thickness δ_2 (mm)	0.14	0.39	1.12
Shape factor H_{12}	4.25	3.17	2.86
Power law exponent N	2.28	6.73	9.07

These three boundary layers were first characterized using the simple power law (Equation 1, and a least-square best fit approximation) and equations 2 to 4. From the power law exponent that best fitted the experimental results, it can be concluded that both boundary layers situated in front of the fin (with and without wing installed) were mostly turbulent, while the one in front of the wing was mostly laminar. The experimental values for the shape factor can be compared to the data from Table I. The results for the fin boundary layer (3.17 and 2.86) compare relatively well to the value from Table I (3.0), supporting the conclusion reached earlier for a turbulent boundary layer. The results for the wing boundary layer (4.25) does not agree as closely with the data from Table I (5.8), which could indicate that the boundary layer is slowly developing into transition (and a less stable boundary layer with a lower shape factor than a fully laminar case).

Another important parameter, the boundary layer thickness, was computed using two different methods: the distance to the wall where the measured velocity equals 0.99 U_∞, and the distance to the wall given by the best fit power law. The boundary layer thickness (δ) calculated with the power law for all three cases present some differences when compared to the values from the experiment. This result demonstrates the difficulty in correlating actual boundary layer thicknesses with exponential methods (asymptotic shape of the boundary layer presents a problem).

Finally, the values of the displacement thickness (δ_1) and of the momentum thickness (δ_2) follow the appropriate trends expected from their definitions. As the boundary layer on the model goes from laminar to turbulent from the front of the wing to the front of the fin, the values of these two characteristics increase accordingly.

As expected, the boundary layer is relatively thin compared to the span of the wings. Thus, this small boundary layer thickness in front of the wing and of the fin (without the wing) means that a large section of the wings surfaces are outside of the boundary layer influence zone (in the undisturbed flow), thus providing large efficient control surfaces. The flow disturbances generated by the presence of the wing on the fin boundary layer are also clearly demonstrated. The thickness of the boundary layer at the fin location corresponds to around 40% of the span of the fins (height of boundary layer is around 18 mm, while the height of the fin is 43.5 mm). However, at a height of 3 mm from the surface of the model, the velocity is already more than 90% of the freestream velocity, thus still providing a relatively large efficient control surface. Finally, an increase in boundary layer thickness is visible as the survey location is moved further downstream.

Analytical calculations (Ref. 3) were performed for the real missile in free-flight in order to provide comparison results. It is not surprising that both locations (free-flight) would yield turbulent boundary layers. The thickness at the front location (in front of the wing) would vary between 10 and 15 mm while it would be between 30 and 35 mm for the location in front of the stability fins (assuming no wing). Calculating the ratio of the boundary layer thickness to the missile body diameter gives a value of δ/d of around 0.07 in front of the wing, and a value of δ/d of around 0.17 in front of the fin. For the present wind tunnel experiment, these values were respectively calculated as being 0.06 and 0.22 (using the measured δ instead of the power law determined value). This should allow for good correlation between free-flight and wind tunnel aerodynamic coefficients as a good similarity exists in the velocity profile and in the relative thickness of the boundary layer between wind tunnel and free-flight conditions.

4.3 Wind Tunnel Results: Mach 3.0

The same locations on the model were used at Mach 3.0 for the measurement of the boundary layer thickness. So, again, 3 sets of results were generated. In front of the wing (a distance of 6.675 calibers from the nose tip), and in front of the fin (a distance of

14.705 calibers from the nose tip). From the present wind tunnel conditions (low Reynolds number), and the positions of the boundary layer surveys, it was calculated that the boundary layer would be laminar at the first location, but turbulent at the second location (Ref. 3). For the first location (laminar), the same analytical calculations forecasted a boundary layer thickness of the order of 0.5 to 2.0 mm.

The data presented in Fig. 7 is for the Mach 3.0 cases (3 sets of data). This information has also been tabulated to allow for easy comparisons. Table III shows various parameters relating to the boundary layer and its development in this high velocity flow.

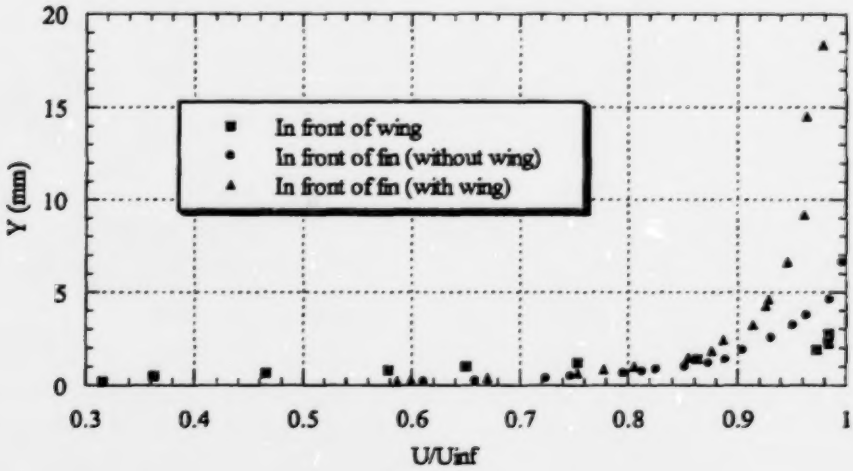

FIGURE 7 – Boundary layer results for Mach 3.0

Again, as with the Mach 2.0 results, these three boundary layers were first characterized using the simple power law (Equation 1, and a least-square best fit approximation) and equations 2 to 4. From the power law exponent that best fitted the experimental results, it can be concluded that both boundary layers situated in front of the fin (with and without wing installed) were mostly turbulent, while the one in front of the wing was mostly laminar. The experimental values for the shape factor can be compared to the data from Table I. Results for the fin boundary layer (5.30 and 4.93) compare relatively well to the value from Table I (5.0), supporting the conclusion reached earlier for a turbulent boundary layer. The results for the wing boundary layer (7.23) does not agree as closely with the data from Table I (9.2). This would indicate that the boundary layer is neither fully laminar nor fully turbulent, but developing into transition (and a less stable boundary layer with a lower shape factor than a fully laminar case).

For the Mach 3.0 boundary layer, the trends and the observations relating to the boundary layer thickness (δ, both experimental and power law values), displacement thickness (δ_1) and momentum thickness (δ_2) are identical to the ones observed at Mach 2.0. Additionally, the results and the conclusions reached from the comparison of the

boundary layer thickness relative to the missile geometry are all identical to that of the Mach 2.0 results (section 4.2).

TABLE III

Boundary layer survey results at Mach 3.0

Parameter	In front of the wing	In front of the fin (without wing)	In front of the fin (both) (with wing)
Boundary layer thickness δ (mm) Experimental	2.73	5.70	18.33
Boundary layer thickness δ (mm) Power Law	2.28	4.11	9.75
Displacement thickness δ_1 (mm)	1.29	1.67	5.96
Momentum thickness δ_2 (mm)	0.18	0.31	1.21
Shape factor H_{12}	7.23	5.30	4.93
Power law exponent N	1.90	7.52	8.93

5.0 CONCLUSIONS AND RECOMMENDATIONS

The driving force behind this investigation was composed of two specific goals. The first one was to compare the boundary layer development at the surface of the model and compare it to the free-flight vehicle. The second one was to validate the accuracy of DREV's wind tunnel in the study of high l/d models with large appendages.

The results from both investigations (Mach 2.0 and 3.0) provided good relative comparisons of boundary layer thickness which should allow for good correlation between free-flight and wind tunnel aerodynamic coefficients.

Comparisons with actual AIM-7M data have shown that DREV's Trisonic Wind Tunnel can provide results comparing well with actual missile bodies. Thus, high l/d bodies with large appendages can successfully be tested in this facility.

6.0 ACKNOWLEDGEMENTS

The author would like to thank Mr. B. Girard for his work in the development of the model and of the testing methodology. The author would also like to thank Messrs. R. Bilodeau and M. Boivin for their assistance with the experimental work. The excellent work of the Prototype Group staff in the fabrication of the models is also greatly acknowledged.

7.0 REFERENCES

1. Fournier, E. Y. and Jeffrey, A. J., "A Computation Fluid Dynamic Analysis of Freestream-Jet Interaction with Application to Reaction-Jet Control on Supersonic Missile Bodies," DREV Technical Memorandum TM-9418, October 1994, UNCLASSIFIED.

2. Fournier, E. Y., "Aerodynamic Coefficients Measurement on a Model of a Sparrow AIM-7M Missile in the DREV Trisonic Wind Tunnel", DREV Technical Memorandum TM-1999-050, July 1999, UNCLASSIFIED.

3. Schlichting, H., "Boundary-Layer Theory", Seventh Edition, McGraw-Hill Book Company, United States, 1987.

4. White, F. M., "Viscous Fluid Flow", McGraw-Hill Book Company, United States, 1974.

BOUNDARY LAYER EXPLORATION
Sparrow model

NOMENCLATURE

Model at 0° ("+" wing configuration)

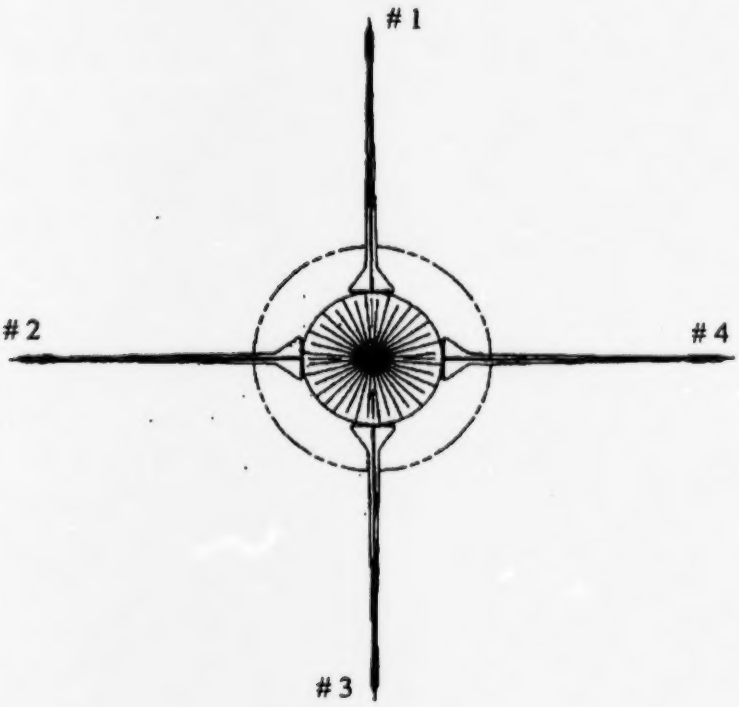

Note : Looking downstream (at the nose of the missile)

BOUNDARY LAYER EXPLORATION: Mach 2.0

Run Number	Y/R	Y	Boundary Layer Location	Model Roll Angle
R6223	0.0127	0.0075	Wing	0° (+)
R6227	0.0169	0.0100	Wing	0° (+)
R6228	0.0254	0.0150	Wing	0° (+)
R6229	0.0296	0.0175	Wing	0° (+)
R6230	0.0339	0.0200	Wing	0° (+)
R6235	0.0423	0.0250	Wing	0° (+)
R6231	0.0491	0.0290	Wing	0° (+)
R6236	0.0593	0.0350	Wing	0° (+)
R6232	0.0677	0.0400	Wing	0° (+)
R6233	0.0677	0.0400	Wing	0° (+)
R6224	0.0804	0.0475	Wing	0° (+)
R6234	0.0957	0.0565	Wing	0° (+)
R6237	0.1270	0.0750	Wing	0° (+)
R6225	0.9441	0.5575	Wing	0° (+)
R6226	2.5758	1.5210	Wing	0° (+)

BOUNDARY LAYER EXPLORATION: Mach 2.0

Run Number	Y/R	Y	Boundary Layer Location	Model Roll Angle
R6238	0.0127	0.0075	Fin	0° (+)
R6239	0.0169	0.0100	Fin	0° (+)
R6240	0.0254	0.0150	Fin	0° (+)
R6241	0.0296	0.0175	Fin	0° (+)
R6242	0.0339	0.0200	Fin	0° (+)
R6243	0.0406	0.0240	Fin	0° (+)
R6244	0.0508	0.0300	Fin	0° (+)
R6245	0.0593	0.0350	Fin	0° (+)
R6246	0.0677	0.0400	Fin	0° (+)
R6247	0.0804	0.0475	Fin	0° (+)
R6248	0.0940	0.0555	Fin	0° (+)
R6249	0.1270	0.0750	Fin	0° (+)
R6250	0.1677	0.0990	Fin	0° (+)
R6251	0.2159	0.1275	Fin	0° (+)
R6252	0.2498	0.1475	Fin	0° (+)
R6253	0.2837	0.1675	Fin	0° (+)
R6254	0.2837	0.1675	Fin	0° (+)
R6255	0.3074	0.1815	Fin	0° (+)
R6256	0.4428	0.2615	Fin	0° (+)

BOUNDARY LAYER EXPLORATION: Mach 2.0

Run Number	Y/R	Y	Boundary Layer Location	Model Roll Angle
R6257	0.0127	0.0075	Fin with Wing	0° (+)
R6258	0.0169	0.0100	Fin with Wing	0° (+)
R6259	0.0254	0.0150	Fin with Wing	0° (+)
R6260	0.0398	0.0235	Fin with Wing	0° (+)
R6261	0.0576	0.0340	Fin with Wing	0° (+)
R6262	0.0677	0.0400	Fin with Wing	0° (+)
R6263	0.0957	0.0565	Fin with Wing	0° (+)
R6264	0.1228	0.0725	Fin with Wing	0° (+)
R6265	0.1693	0.1000	Fin with Wing	0° (+)
R6266	0.2159	0.1275	Fin with Wing	0° (+)
R6267	0.2837	0.1675	Fin with Wing	0° (+)
R6268	0.2837	0.1675	Fin with Wing	0° (+)
R6269	0.3074	0.1815	Fin with Wing	0° (+)
R6270	0.3074	0.1815	Fin with Wing	0° (+)
R6271	0.4428	0.2615	Fin with Wing	0° (+)
R6272	0.6122	0.3615	Fin with Wing	0° (+)
R6273	0.9678	0.5715	Fin with Wing	0° (+)
R6274	1.2218	0.7215	Fin with Wing	0° (+)

BOUNDARY LAYER EXPLORATION: Mach 3.0

Run Number	Y/R	Y	Boundary Layer Location	Model Roll Angle
R6308	0.0127	0.0075	Wing	0° (+)
R6320	0.0254	0.0150	Wing	0° (+)
R6319	0.0322	0.0190	Wing	0° (+)
R6318	0.0423	0.0250	Wing	0° (+)
R6317	0.0533	0.0315	Wing	0° (+)
R6316	0.0652	0.0385	Wing	0° (+)
R6310	0.0804	0.0475	Wing	0° (+)
R6315	0.0923	0.0545	Wing	0° (+)
R6314	0.1262	0.0745	Wing	0° (+)
R6312	0.1490	0.0880	Wing	0° (+)
R6313	0.1820	0.1075	Wing	0° (+)

BOUNDARY LAYER EXPLORATION: Mach 3.0

Run Number	Y/R	Y	Boundary Layer Location	Model Roll Angle
R6292	0.0127	0.0075	Fin	0° (+)
R6293	0.0169	0.0100	Fin	0° (+)
R6294	0.0254	0.0150	Fin	0° (+)
R6295	0.0322	0.0190	Fin	0° (+)
R6296	0.0423	0.0250	Fin	0° (+)
R6297	0.0500	0.0295	Fin	0° (+)
R6298	0.0576	0.0340	Fin	0° (+)
R6299	0.0660	0.0390	Fin	0° (+)
R6300	0.0804	0.0475	Fin	0° (+)
R6301	0.0923	0.0545	Fin	0° (+)
R6302	0.1270	0.0750	Fin	0° (+)
R6303	0.1702	0.1005	Fin	0° (+)
R6304	0.2159	0.1275	Fin	0° (+)
R6305	0.2498	0.1475	Fin	0° (+)
R6306	0.3074	0.1815	Fin	0° (+)
R6307	0.4428	0.2615	Fin	0° (+)

BOUNDARY LAYER EXPLORATION: Mach 3.0

Run Number	Y/R	Y	Boundary Layer Location	Model Roll Angle
R6275	0.0127	0.0075	Fin with Wing	0° (+)
R6276	0.0169	0.0100	Fin with Wing	0° (+)
R6277	0.0246	0.0145	Fin with Wing	0° (+)
R6278	0.0423	0.0250	Fin with Wing	0° (+)
R6279	0.0423	0.0250	Fin with Wing	0° (+)
R6280	0.0550	0.0325	Fin with Wing	0° (+)
R6281	0.0660	0.0390	Fin with Wing	0° (+)
R6282	0.0982	0.0580	Fin with Wing	0° (+)
R6283	0.1219	0.0720	Fin with Wing	0° (+)
R6284	0.1609	0.0950	Fin with Wing	0° (+)
R6285	0.2159	0.1275	Fin with Wing	0° (+)
R6286	0.2837	0.1675	Fin with Wing	0° (+)
R6287	0.3074	0.1815	Fin with Wing	0° (+)
R6288	0.4428	0.2615	Fin with Wing	0° (+)
R6289	0.6122	0.3615	Fin with Wing	0° (+)
R6290	0.9678	0.5715	Fin with Wing	0° (+)
R6291	1.2218	0.7215	Fin with Wing	0° (+)

APPENDIX B

Detailed Drawings of Model

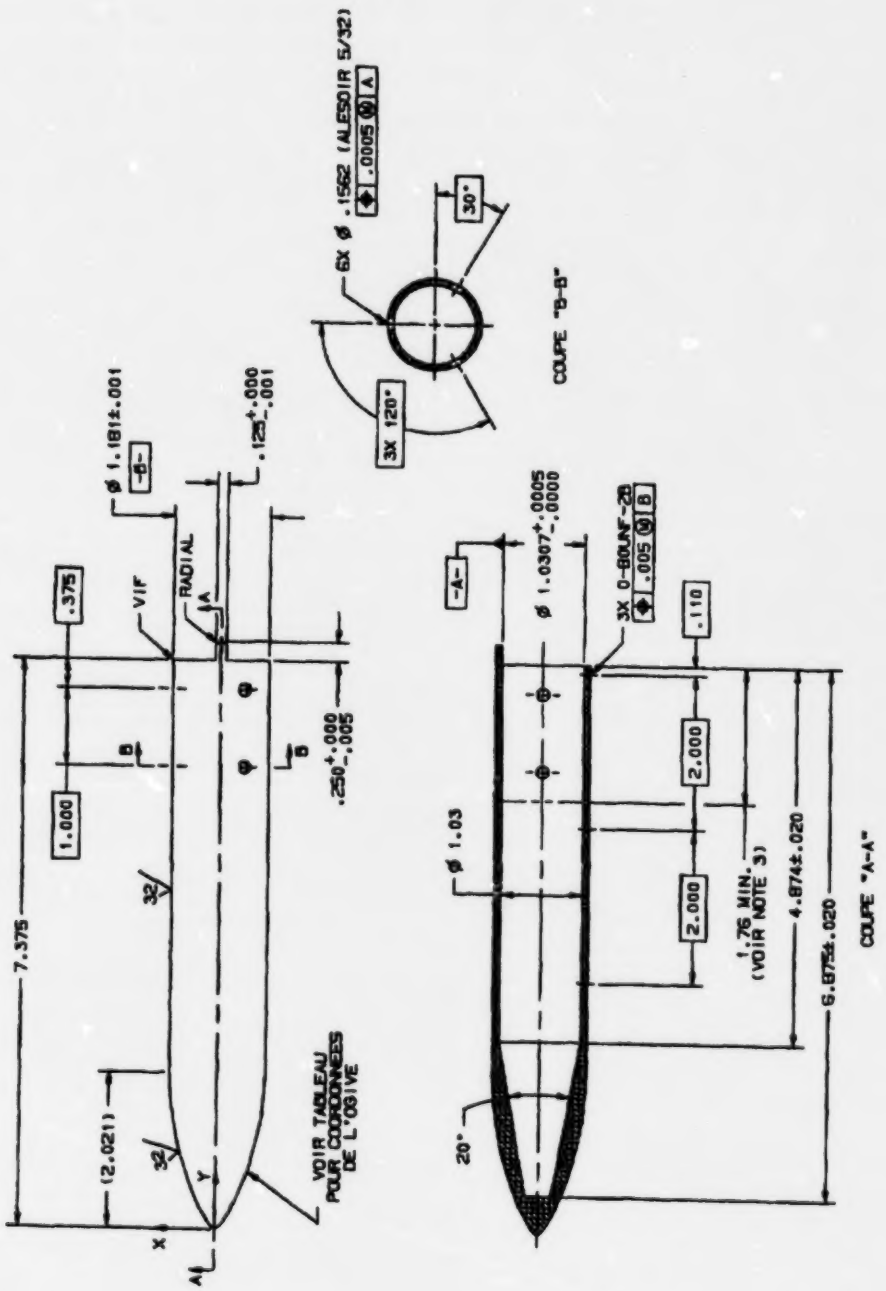

FIGURE B-1 – Sparrow model nose/forebody module (dimensions in inches)

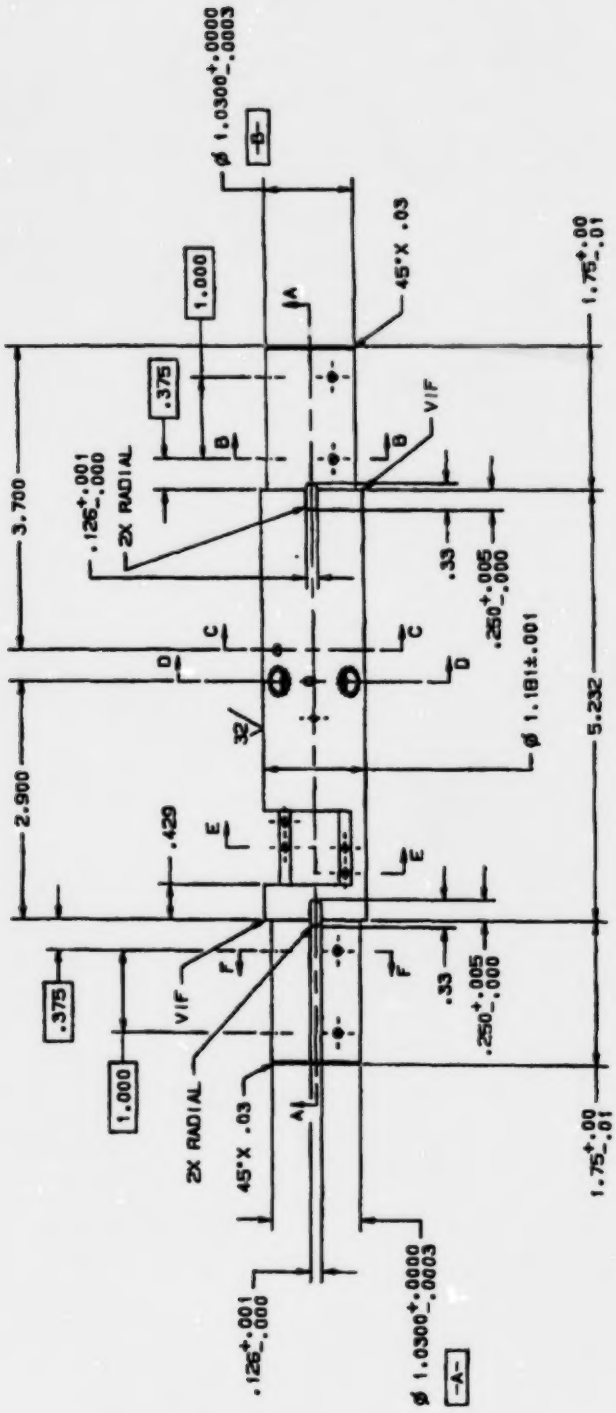

FIGURE B-2 – Sparrow model central body module, with control fins attachment holes (dimensions in inches)

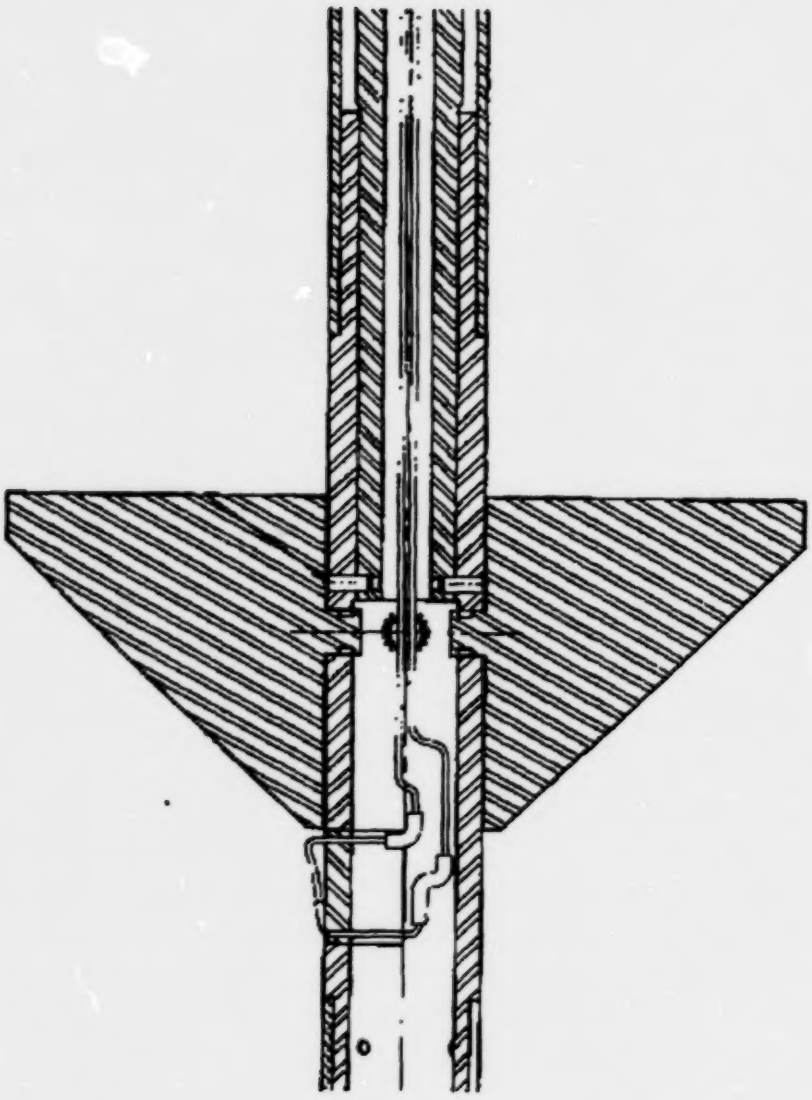

FIGURE B-3 – Sparrow model central body module used for aerodynamic studies (general arrangement)

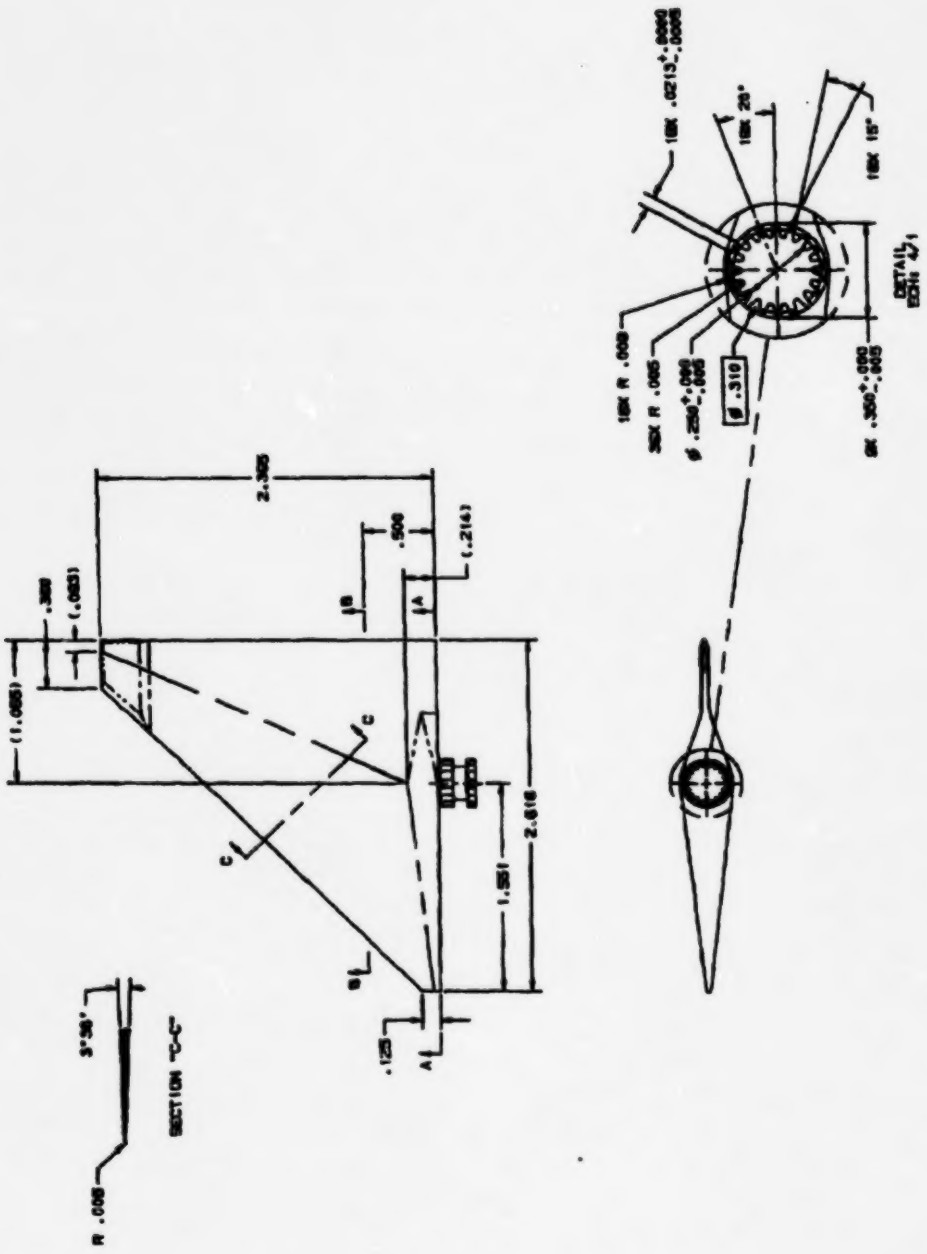

FIGURE B-4 – Sparrow model control fins (dimensions in inches)

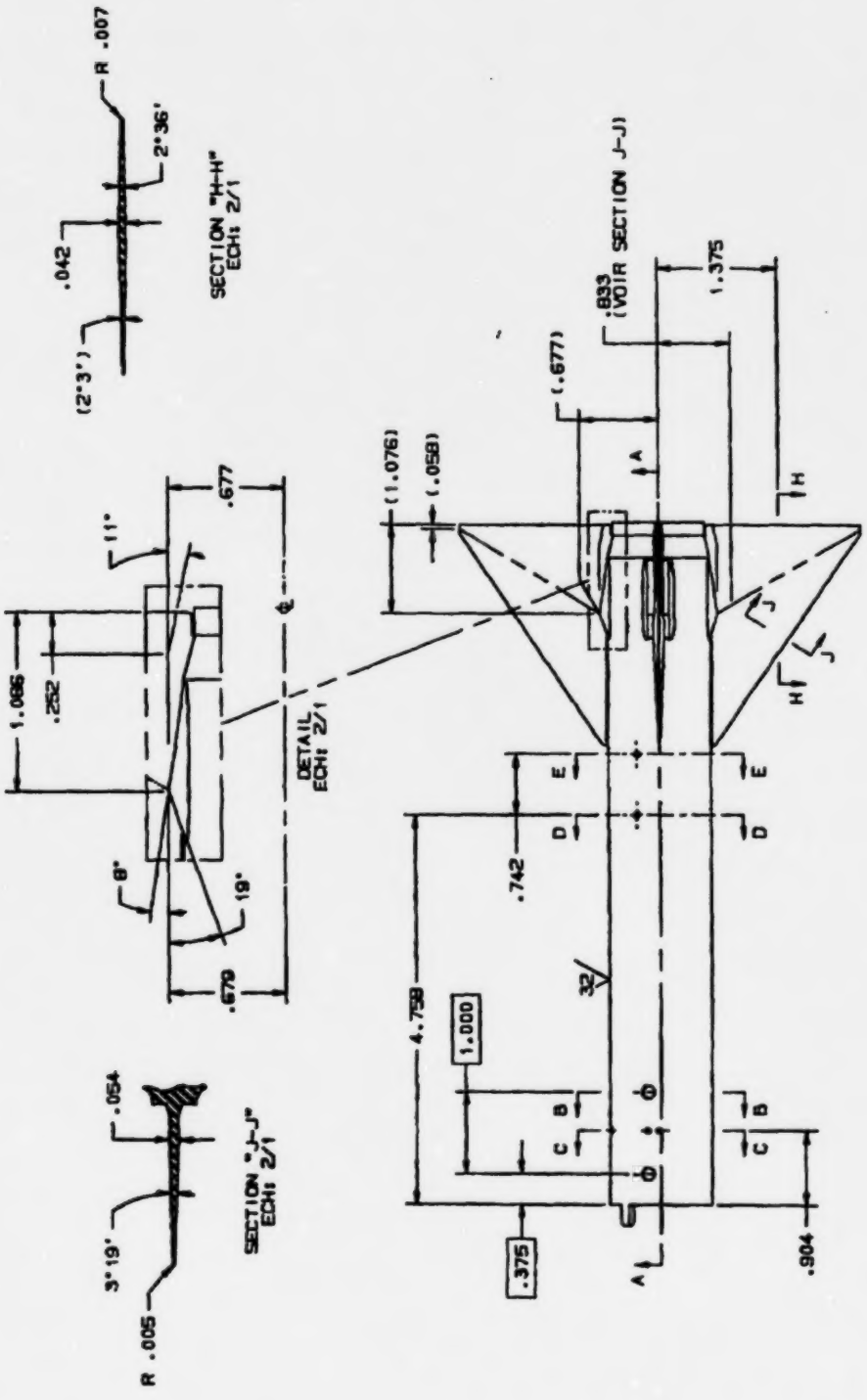

FIGURE B-5 – Sparrow model after-body module, with tail fins
(dimensions in inches)

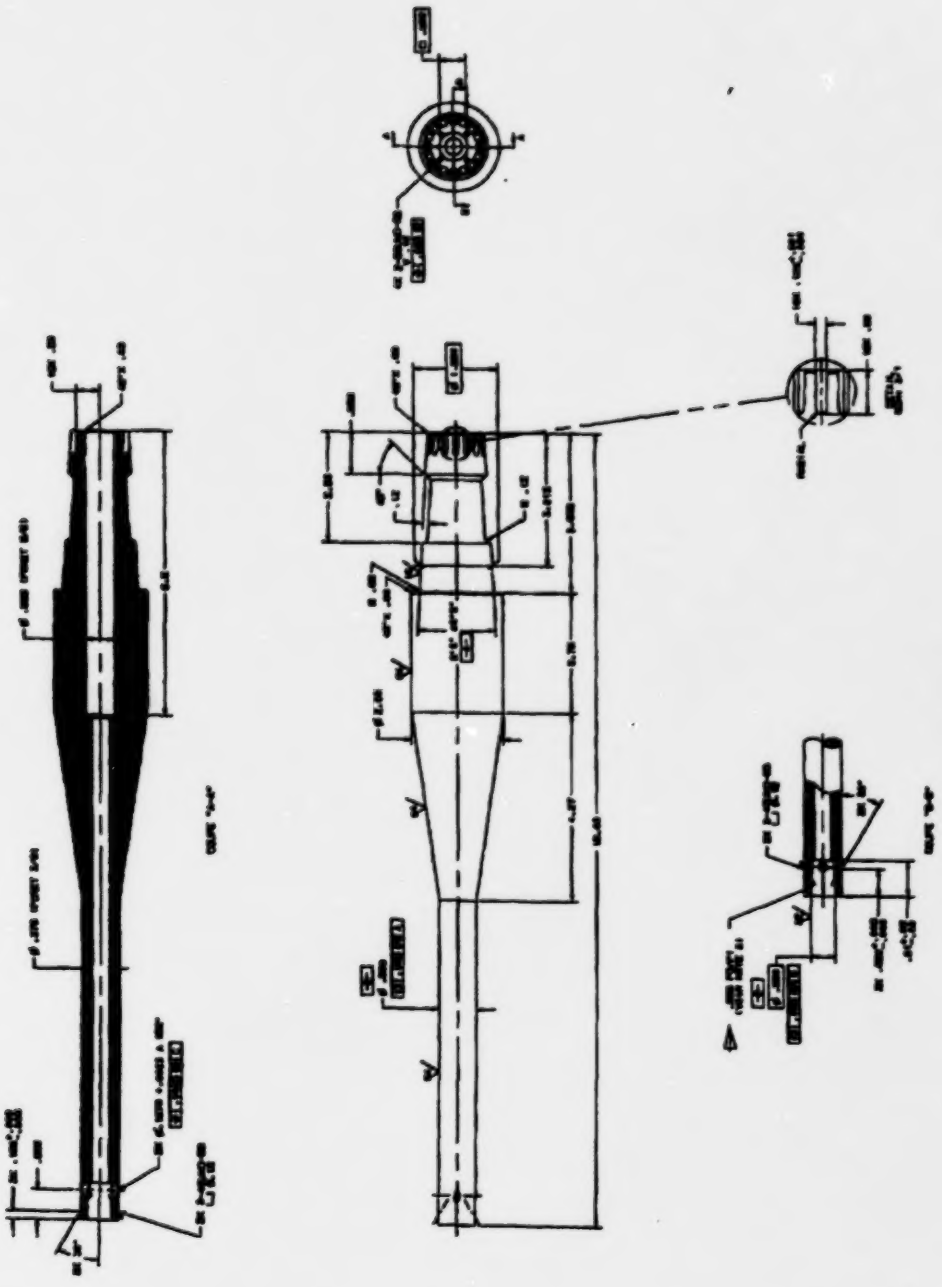

FIGURE B-6 – Balance (0.75 in) sting holder (dimensions in inches)